The vapour–liquid transition of charge-stabilized colloidal suspensions: an effective one-component description

2003 J. Phys.: Condens. Matter 15 S3537

(http://iopscience.iop.org/0953-8984/15/48/013)

INSTITUTE OF PHYSICS PUBLISHING JOURNAL OF PHYSICS: CONDENSED MATTER

J. Phys.: Condens. Matter **15** (2003) S3537–S3547 PII: S0953-8984(03)66485-4

The vapour–liquid transition of charge-stabilized colloidal suspensions: an effective one-component description

G Ruiz[1], **J A Anta**[2] **and C F Tejero**[3]

[1] EUIT Aeronáuticos, Universidade Politécnica de Madrid, E-28040 Madrid, Spain
[2] Departamento de CC. Ambientales, Universidade Pablo de Olavide, E-41013 Sevilla, Spain
[3] Facultad de CC. Físicas, Universidade Complutense, E-28040 Madrid, Spain

E-mail: cftejero@fis.ucm.es

Received 21 July 2003
Published 20 November 2003
Online at stacks.iop.org/JPhysCM/15/S3537

Abstract

The low-density phase diagrams of charge-stabilized colloidal suspensions of the Derjaguin–Landau–Verwey–Overbeek theory with an approximate effective one-component Hamiltonian given by the volume term and effective pair interactions, and of the classical theory (without including the volume term), are obtained from the hypernetted-chain integral equation at low colloidal charges. In the salt-free case both phase diagrams exhibit a vapour–liquid transition with short-ranged colloid–colloid correlations. This phase separation is compared to the vapour–liquid transition found in binary mixtures of highly asymmetrical hard spheres.

1. Introduction

The archetypal model of a colloidal dispersion is an aqueous suspension of colloidal (mesoscopic) particles with ionizable groups on their surface [1]. When they are dispersed in a polar liquid such as water, some of the ionizable groups dissociate and colloidal particles acquire an electric charge. Since the discharged counterions remain near the charged colloidal particles, the result is the formation of an electric double layer surrounding the particles, composed of the counterions and the ions of any salt added to the suspension. When two colloidal particles approach each other, the overlap of these double layers causes an effective repulsive force between the particles.

The mesoscopic size of the colloidal particles yields to characteristic length scales which are widely separated from those of the small microions. Hence it seems natural to reduce the multicomponent system into an effective one-component description involving only the mesoscopic particles. This can be formally done by tracing out in the partition function of the multicomponent system the coordinates and momenta of the microions leading to an

exact effective one-component Hamiltonian for the mesoscopic particles which contains the kinetic energy, the colloid–colloid direct interactions and a free-energy term [2]. By its construction, the reduction to an exact effective one-component Hamiltonian preserves the average value of the two-particle density dynamical function, i.e. the colloid–colloid pair correlation function (pcf). Since the complexity of the multicomponent system with different length scales is conserved in the exact effective one-component Hamiltonian, one needs to resort to approximations in order to obtain a tractable expression for this quantity.

An approximate effective one-component Hamiltonian for an aqueous suspension of spherical colloidal particles, of radius R and charge $-Ze$ uniformly distributed over the particle surface, and point-particle microions (counterions of charge $+e$ and fully dissociated pairs of monovalent salt ions of charge $\pm e$, which cannot penetrate the interior of the colloidal particles) has recently been obtained within a mean-field density-functional approach [3]. The solvent is assumed to be a continuum of dielectric constant ϵ and the multicomponent Hamiltonian consists of short-ranged (hard-sphere) repulsions and long-ranged Coulombic interactions. The above analysis leads to an approximate effective one-component Hamiltonian:

$$H = F_0(N, V, T) + \frac{1}{2M}\sum_{j=1}^{N}\mathbf{P}_j^2 + \frac{1}{2}\sum_{i=1}^{N}\sum_{i\neq j=1}^{N} V(|\mathbf{R}_i - \mathbf{R}_j|; \rho, T), \tag{1}$$

where $\mathbf{R}_j$ and $\mathbf{P}_j$ ($j = 1, 2, \ldots, N$) are the coordinates and momenta of the colloidal particles of mass M, $F_0(N, V, T)$ is the volume term (with N the colloidal particle number, V the volume, and T the temperature), and $V(r; \rho, T)$, with $\rho = N/V$, is the Derjaguin–Landau–Verwey–Overbeek (DLVO) potential [4],

$$V(r; \rho, T) = V_{\mathrm{HS}}(r) + \frac{Z^2e^2}{\epsilon}\left(\frac{\mathrm{e}^{\kappa R}}{1+\kappa R}\right)^2\frac{\mathrm{e}^{-\kappa r}}{r}\Theta(r - 2R). \tag{2}$$

In (2) r is the interparticle distance, $V_{\mathrm{HS}}(r)$ is the hard-sphere potential for particles of radius R, $\Theta(x)$ is the Heaviside function and κ is the Debye screening parameter:

$$\kappa^2 = \frac{4\pi e^2}{\epsilon k_{\mathrm{B}}T}(Z\rho + 2\rho_{\mathrm{s}}), \tag{3}$$

with k_{B} the Boltzmann constant and ρ_{s} the density of the ions of an added monovalent salt. We note that in (1) the effect of microion-mediated interactions between the colloidal particles, which are present in the multicomponent Hamiltonian, is manifested via the volume term and effective state-dependent interactions.

Although accurate measurements on a pair of charge-stabilized colloidal particles show nothing but a pure repulsion in quantitative agreement with the DLVO potential [5], the existence in the bulk of a vapour–liquid transition at extremely low salt concentrations has been the subject of controversy in recent years [6]. In this paper we are concerned with the low-density phase diagram resulting from the DLVO theory (1) and from the classical DLVO theory (without including the volume term) at low colloidal charges.

2. A self-consistent thermodynamics

The lack in (1) of all n-particle ($n \geqslant 3$) effective interactions is, indeed, an approximation. Note that the short-ranged colloid–colloid pcf $g(r; \rho, T)$ resulting from (1) only stems from the repulsive DLVO potential. The reason for this is that the volume term and the kinetic energy cancel in the average value of the two-particle density dynamical function. Although $g(r; \rho, T)$ differs from the colloid–colloid pcf in the multicomponent system, the main advantage of the effective pair potential approximation seems to be that the well known equations that relate

the structure to the thermodynamics for atomic pair potentials can be easily transposed to the effective one-component description.

Let us denote by $F(N, V, T)$ the Helmholtz free energy in the effective one-component description (1), i.e.

$$F(N, V, T) = F_0(N, V, T) + F^{\mathrm{id}}(N, V, T) + F^{\mathrm{ex}}(N, V, T), \tag{4}$$

where $F^{\mathrm{id}}(N, V, T)$ and $F^{\mathrm{ex}}(N, V, T)$ are the ideal and the excess parts of the Helmholtz free energy of a system of particles interacting with the DLVO potential. We note that $F^{\mathrm{ex}}(N, V, T)$ depends, as for atomic systems, on N, V and T (explicit dependences) but also includes additional N, V and T dependences (implicit dependences) induced through the DLVO potential. When the excess contribution is viewed as a functional of the pair potential $F^{\mathrm{ex}}(N, V, T) \equiv F^{\mathrm{ex}}[V(r; \rho, T)]$, the two-particle density $\rho_2(\mathbf{r}, \mathbf{r}'; \rho, T)$ is

$$\rho_2(\mathbf{r}, \mathbf{r}'; \rho, T) = 2\frac{\delta F^{\mathrm{ex}}[V(|\mathbf{r} - \mathbf{r}'|; \rho, T)]}{\delta V(|\mathbf{r} - \mathbf{r}'|; \rho, T)}, \tag{5}$$

which is a simple transposition of the well known equation for state-independent pair potentials [7], since ρ and T appear in $V(r; \rho, T)$ as parameters. Integrating (5) following a linear path of integration $\alpha V(r; \rho, T)$ ($0 \leqslant \alpha \leqslant 1$) between the ideal gas ($\alpha = 0$) and the actual fluid ($\alpha = 1$) and taking into account that for a uniform phase $\rho_2(r; \rho, T) = \rho^2 g(r; \rho, T)$, the free energy per particle in the thermodynamic limit reads

$$f(\rho, T) = f_0(\rho, T) + k_{\mathrm{B}}T[\ln(\rho\Lambda^3) - 1] + \tfrac{1}{2}\rho \int_0^1 \mathrm{d}\alpha \int \mathrm{d}\mathbf{r}\, g(r; \rho, T|\alpha) V(r; \rho, T), \tag{6}$$

where $f_0(\rho, T) = F_0(T, V, N)/N$, Λ is the thermal de Broglie wavelength of the colloidal particles and $g(r; \rho, T|\alpha)$ denotes the pcf for the fluid with potential $\alpha V(r; \rho, T)$.

From the thermodynamic relations,

$$p(\rho, T) = \rho^2 \frac{\partial f(\rho, T)}{\partial \rho}; \qquad u(\rho, T) = f(\rho, T) - T\frac{\partial f(\rho, T)}{\partial T}, \tag{7}$$

where $p(\rho, T)$ is the pressure and $u(\rho, T)$ is the internal energy per particle, we obviously conclude that because of the implicit dependences neither the virial equation nor the energy equation for atomic fluids hold in the effective one-component description. From (6) and (7), a standard calculation yields the equation of state:

$$p(\rho, T) = p_0(\rho, T) + \rho k_{\mathrm{B}}T - \frac{1}{6}\rho^2 \int \mathrm{d}\mathbf{r}\, g(r; \rho, T) r \frac{\partial}{\partial r} V_{\mathrm{p}}(r; \rho, T), \tag{8}$$

where $p_0(\rho, T)$ is the contribution of the volume term,

$$V_{\mathrm{p}}(r; \rho, T) = V_{\mathrm{HS}}(r) + \bar{V}_{\mathrm{p}}(r; \rho, T)\Theta(r - 2R), \tag{9}$$

and

$$\bar{V}_{\mathrm{p}}(r; \rho, T) = \frac{Z^2 e^2}{\epsilon}\left(\frac{\mathrm{e}^{\kappa R}}{1 + \kappa R}\right)^2 \frac{3\kappa^2 R^2}{1 + \kappa R}\left[\frac{\mathrm{e}^{-\kappa r}}{r} - \kappa\Gamma(0, \kappa r)\right] + \frac{Z^2 e^2}{\epsilon}\left(\frac{\mathrm{e}^{\kappa R}}{1 + \kappa R}\right)^2 \left[\frac{\mathrm{e}^{-\kappa r}}{r} - \frac{3}{2}\kappa\Gamma(0, \kappa r)\right], \tag{10}$$

where $\Gamma(0, x) = \int_x^\infty \mathrm{d}t\, t^{-1}\mathrm{e}^{-t}$ is the incomplete gamma function. We point out that the last two terms in (8) are nothing but an exact transformation of the Ascarelli–Harrison equation of state first applied to the case of liquid metals [8].

From (6) and (7) the energy equation reads

$$u(\rho, T) = u_0(\rho, T) + \tfrac{3}{2}k_{\mathrm{B}}T + \tfrac{1}{2}\rho \int \mathrm{d}\mathbf{r}\, g(r; \rho, T) V_{\mathrm{u}}(r; \rho, T), \tag{11}$$

where $u_0(\rho, T)$ is the contribution of the volume term,

$$V_{\mathrm{u}}(r;\rho,T) = V_{\mathrm{HS}}(r) + \bar{V}_{\mathrm{u}}(r;\rho,T)\Theta(r-2R), \tag{12}$$

and

$$\bar{V}_{\mathrm{u}}(r;\rho,T) = \frac{Z^2e^2}{\epsilon}\left(\frac{\mathrm{e}^{\kappa R}}{1+\kappa R}\right)^2\left(1+\frac{\kappa^2R^2}{1+\kappa R}\right)\frac{\mathrm{e}^{-\kappa r}}{r} - \frac{Z^2e^2}{2\epsilon}\left(\frac{\mathrm{e}^{\kappa R}}{1+\kappa R}\right)^2\kappa\mathrm{e}^{-\kappa r}. \tag{13}$$

The last two terms in the rhs of (6), (8) and (11) look like the free energy, the virial and the energy equations for atomic fluids but with different state-dependent potentials. Although the structure and the complete thermodynamics results from the DLVO potential, it could be said that the structure is determined from $V(r;\rho,T)$, the phase diagram from $V_{\mathrm{p}}(r;\rho,T)$ and the internal energy from $V_{\mathrm{u}}(r;\rho,T)$. The new potentials $V_{\mathrm{p}}(r;\rho,T)$ and $V_{\mathrm{u}}(r;\rho,T)$ guarantee a self-consistent thermodynamics in the effective one-component description. We also note that from $V_{\mathrm{p}}(r;\rho,T)$ or $V_{\mathrm{u}}(r;\rho,T)$ neither the structure nor the complete thermodynamics can be reproduced.

3. The Debye–Hückel fluid

We first consider the case of point particles ($R = 0$) without including the volume term. The phase diagram for particles interacting with the Debye–Hückel pair potential has been extensively studied in the literature. From (2), (10) and (13) we have

$$V(r;\rho,T) = \frac{Z^2e^2}{\epsilon}\frac{\mathrm{e}^{-\kappa r}}{r}, \tag{14}$$

$$V_{\mathrm{p}}(r;\rho,T) = \frac{Z^2e^2}{\epsilon}\left[\frac{\mathrm{e}^{-\kappa r}}{r} - \frac{3}{2}\kappa\Gamma(0,\kappa r)\right], \tag{15}$$

and

$$V_{\mathrm{u}}(r;\rho,T) = \frac{Z^2e^2}{\epsilon}\left[\frac{\mathrm{e}^{-\kappa r}}{r} - \frac{1}{2}\kappa\mathrm{e}^{-\kappa r}\right], \tag{16}$$

that is, despite the purely repulsive nature of the Debye–Hückel potential, both $V_{\mathrm{p}}(r;\rho,T)$ and $V_{\mathrm{u}}(r;\rho,T)$ contain an attractive contribution.

Computer simulations [9] show that in the high-salt limit $2\rho_{\mathrm{s}} \gg Z\rho$ the phase diagram contains three phases, namely fluid, a body-centred cubic (bcc) crystal, and a face-centred cubic (fcc) crystal, the full phase diagram consisting of two melting lines (fluid–bcc and fluid–fcc) and a structural transition (bcc–fcc). In the low-salt limit $2\rho_{\mathrm{s}} \ll Z\rho$ the phase diagram obtained from Monte Carlo simulations contains a vapour–liquid transition [10], while no evidence for a stable crystalline phase is found. This phase separation, in a fluid with purely repulsive forces, does not escape however the classical van der Waals picture since the phase diagram results from $V_{\mathrm{p}}(r;\rho,T)$ which contains a long-ranged attraction. Since $V_{\mathrm{p}}(r;\rho;T) > 0$ ($r < r_0$) and $V_{\mathrm{p}}(r;\rho;T) < 0$ ($r > r_0$), with $\kappa r_0 \simeq 1.45$, when the salt density increases the repulsions are favoured over the attractions; that is, the addition of salt lowers the vapour–liquid critical point, favouring the fluid phase in the phase diagram. This can be easily shown within a mean-field approach, i.e. $g(r;\rho,T) \simeq 0$ for $r < a$, with a the average interparticle distance $a^3 = 1/\rho$, and $g(r;\rho,T) \simeq 1$ for $r > a$. We use as independent variables the charge number Z (Z^{-2} playing the role of the temperature T) and $q = \kappa a$ (with q^{-3} the average number of particles in a cubic box of length κ^{-1}), while $\xi = 2\rho_{\mathrm{s}}/Z\rho$ is treated as a free parameter. The phase diagram resulting from (8) and (15) exhibits a vapour–liquid transition, the critical point being located at $Z_{\mathrm{c}} = 21.6$ and $q_{\mathrm{c}} = 1.73$ for $\xi = 0$ and at $Z_{\mathrm{c}} = 305.6$ and $q_{\mathrm{c}} = 6.61$ for $\xi = 0.25$.

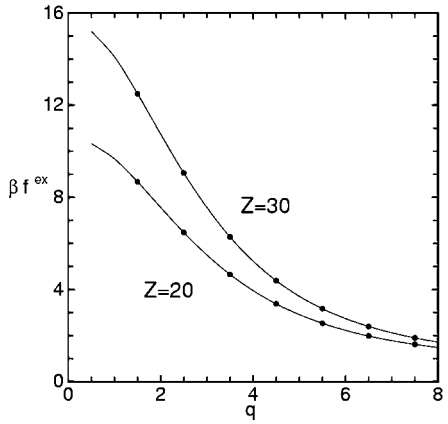

Figure 1. Reduced excess free energy per particle $\beta f^{\rm ex} \equiv \beta f^{\rm ex}(\rho, T)$ versus q of the Debye–Hückel fluid as obtained from HNC (full curve) and from thermodynamical integration of the virial equation (full dots) for $Z = 20$ and 30.

We observe that when ξ changes from $\xi = 0$ to 0.25 the Debye screening parameter increases by a factor of 1.12 whereas the critical temperature decreases by a factor of 5×10^{-3}; i.e. the addition of salt dramatically lowers the critical temperature.

To end this section we consider the salt-free case $\xi = 0$. The structure has been determined from the hypernetted-chain (HNC) integral equation:

$$\ln g(r;\rho,T) = -\beta V(r;\rho,T) + h(r;\rho,T) - c(r;\rho,T), \tag{17}$$

with $c(r;\rho,T)$ the direct correlation function (dcf) and $h(r;\rho,T) = g(r;\rho,T) - 1$ the total correlation function (tcf). Within the HNC integral equation the excess free energy $f^{\rm ex}(\rho,T)$ can be expressed in terms of the tcf, the dcf and their Fourier transforms $\tilde{h}(k;\rho,T)$ and $\tilde{c}(k;\rho,T)$ [11]:

$$\beta f^{\rm ex}(\rho,T) = \frac{1}{2}\rho \int {\rm d}\mathbf{r}\, A(r;\rho,T) + \frac{1}{16\pi^3\rho}\int {\rm d}\mathbf{k}\, B(k;\rho,T), \tag{18}$$

where

$$A(r;\rho,T) = c(r;\rho,T) + h(r;\rho,T)[c(r;\rho,T) - \tfrac{1}{2}h(r;\rho,T)], \tag{19}$$

and

$$B(k;\rho,T) = \ln[1 - \rho\tilde{c}(k;\rho,T)] + \rho\tilde{h}(k;\rho,T). \tag{20}$$

From the virial and the energy equations $f^{\rm ex}(\rho,T)$ can also be obtained by thermodynamical integration of (7)[Note 4]. In figures 1 and 2 the high degree of thermodynamical consistency of the HNC route and the virial and the energy routes is shown. In figure 3 the phase diagrams in the (q, Z) plane as obtained from mean-field theory, i.e.

$$\beta p(\rho,T) = \rho[1 - \tfrac{1}{12}Zq^2{\rm e}^{-q}], \tag{21}$$

with $q = \sqrt{4\pi\lambda Z\rho}a$ and $\lambda = e^2/\epsilon k_{\rm B}T$ the Bjerrum length, and from the HNC integral equation are compared to the Monte Carlo simulation results by Dijkstra and van Roij [10]. Note that although the lack of attractions in $V(r;\rho,T)$ precludes the divergence of correlations, the HNC integral equation captures a vapour–liquid transition indicating that the density dependence of the Debye–Hückel potential is responsible for driving the fluid towards the phase separation.

[4] In each case the integration constant can be separately set equal to zero.

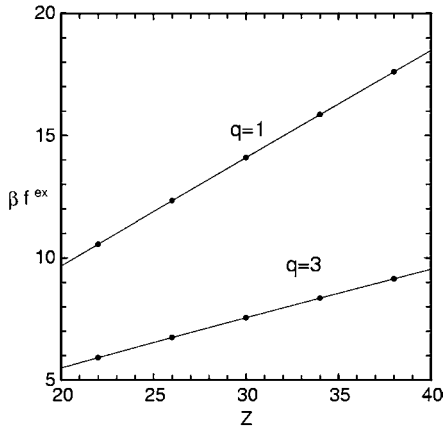

Figure 2. Reduced excess free energy per particle $\beta f^{\rm ex} \equiv \beta f^{\rm ex}(\rho, T)$ versus Z of the Debye–Hückel fluid as obtained from HNC (full curve) and from thermodynamical integration of the energy equation (full dots) for $q = 1$ and 3.

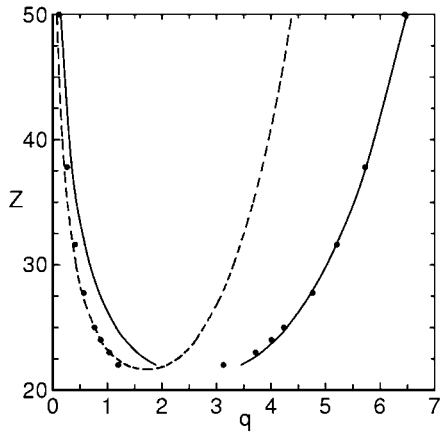

Figure 3. Phase diagram in the q–Z plane of the Debye–Hückel fluid as obtained from mean-field theory (broken curve) and from HNC (full curve). The full dots denote the Monte Carlo simulation results by Dijkstra and van Roij.

This somewhat academic problem[5] illustrates that the thermodynamic states for which the compressibility diverges are not associated in the effective one-component description with long-ranged correlations. As explained elsewhere, the thermodynamical self-consistency implies that the compressibility equation for atomic fluids has also to be modified for density-dependent interactions [12].

4. Binary mixtures versus HNC–DLVO

Salt-free binary mixtures of highly asymmetrical charged hard spheres are known to exhibit a phase separation at very low concentrations [13]. In this section the structure and the

[5] Inside the coexistence curve the phase diagram exhibits a region of negative pressures which contains the liquid spinodal. These anomalous properties can be analytically determined within the mean-field approach (21).

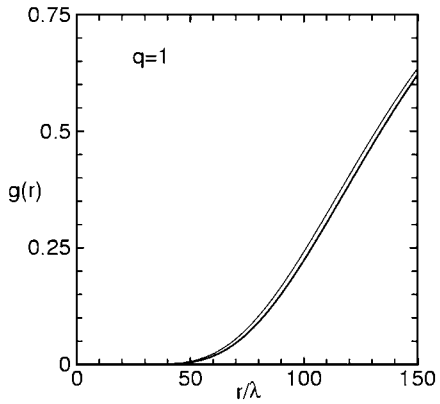

Figure 4. Colloid–colloid pcf $g(r) \equiv g(r; \rho, T)$ versus the reduced distance r/λ for $Z = 20$, $R/\lambda = 2.5$ and $q = 1$ as obtained from the classical HNC–DLVO (full curve) and from CGHNC (thin full curve).

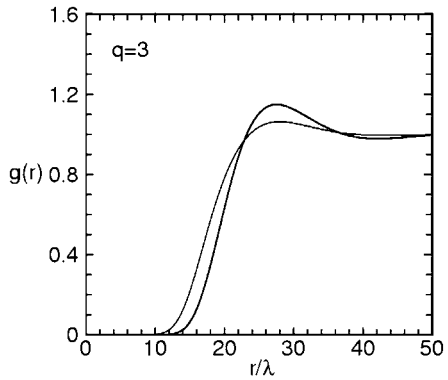

Figure 5. The same as in figure 4 for $q = 3$.

thermodynamics of a binary mixture of hard-sphere colloidal particles of radius R and charge $-Ze$ and point-particle monovalent counterions are obtained using a recently proposed coarse-graining hypernetted-chain (CGHNC) integral equation approach [14]. This procedure is designed to obtain efficiently the colloid–colloid structure and effective pair potentials starting from a multicomponent description. The results are compared to HNC (17)–(20), with $V(r; \rho, T)$ the DLVO potential, in the salt-free case effective one-component description (1).

In figures 4–6 we plot the colloid–colloid pcf as obtained from CGHNC and from the classical (without including the volume term) HNC–DLVO as a function of the reduced distance r/λ for $Z = 20$ and $R/\lambda = 2.5$ at several densities. It is seen that at $q = 1$ and 5.8 both approaches agree quite well. However, in the vicinity of the classical HNC–DLVO critical region $q = 3$ (see figure 7) significant differences are found.

In figure 7 the phase diagram in the q–Z plane as obtained from the classical HNC–DLVO theory and from the HNC–DLVO theory is shown. In the salt-free case, the contribution of the volume term to the pressure in (8) is given by

$$p_0(\rho, T) = Z\rho k_B T\left[1 - \frac{1}{4}Z\frac{\kappa R}{(1+\kappa R)^2}\left(\frac{\lambda}{R}\right)\right], \tag{22}$$

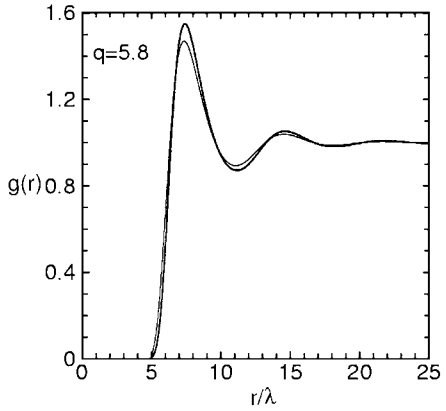

Figure 6. The same as in figure 4 for $q = 5.8$.

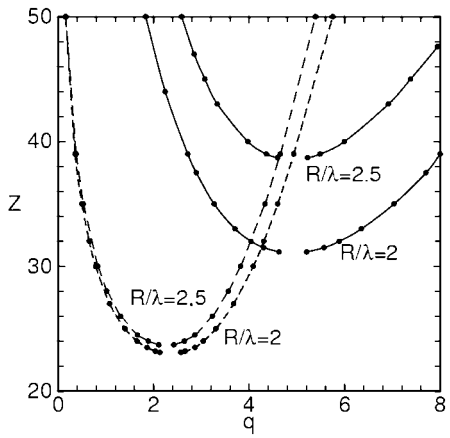

Figure 7. Phase diagram in the q–Z plane of the HNC–DLVO fluid (full dots and full curve) and of the classical HNC–DLVO fluid (full dots and broken curve) for $R/\lambda = 2$ and 2.5.

which consists of the ideal gas pressure of the counterions and the contribution coming from the self-energy of the N electric double layers associated with the individual mesoscopic particles [3]. In both cases, a vapour–liquid transition is found. Moreover, it is seen that the volume term shifts the critical point to higher Z and q and that by increasing R/λ the volume term dominates the phase separation, the density-dependent screening DLVO mechanism playing only a minor role. Within the CGHNC we have been unable to obtain the coexistence region since at very low densities the correlations become long ranged and convergence problems arise.

In figure 8 the normalized isothermal compressibility of the CGHNC is compared to HNC–DLVO for $R/\lambda = 2.5$. It is seen that at low charges the effective one-component description is a quite good approximation but fails as Z increases. In all cases HNC–DLVO underestimates the isothermal compressibility.

In figure 9 the HNC–DLVO phase diagram in the η–R/λ plane is shown for $Z = 10$, 15 and 20. It is seen that the critical packing fraction seems to be nearly independent of Z ($\eta_c \simeq 0.006$) and that the critical radius R_c/λ is nearly linear in Z. Our findings are in qualitative agreement with [13].

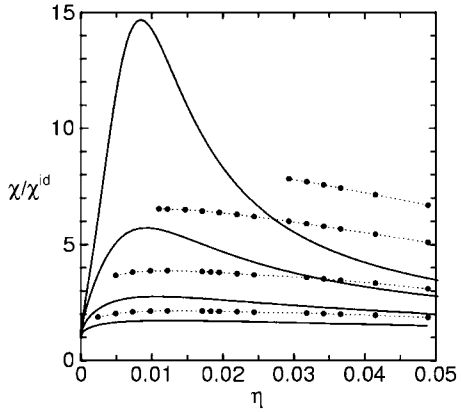

Figure 8. Reduced isothermal compressibility χ/χ^{id} versus the colloid packing fraction η for $R/\lambda = 2.5$ as obtained from HNC–DLVO (full curve) and from CGHNC (full dots and broken curve) for (from bottom to top) $Z = 17, 25, 32$ and 36.

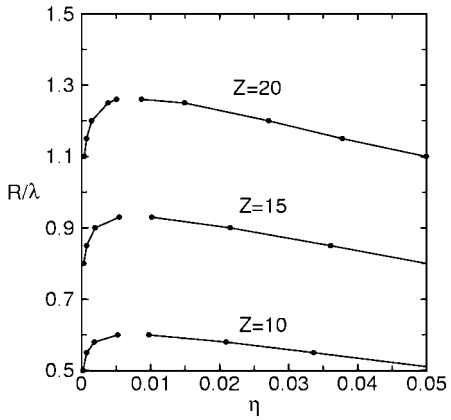

Figure 9. Phase diagram in the η–R/λ plane of the HNC–DLVO fluid for $Z = 10$, 15 and 20.

5. Conclusions

The existence in the bulk of an effective attraction between like-charged colloidal particles in a binary mixture of highly asymmetrical charged hard spheres is controversial [15]. In the salt-free case this effective attraction would yield a vapour–liquid transition and, according to the compressibility equation, the approach of the critical point would imply long-ranged colloid–colloid pcf. When the mixture is replaced by an effective one-component description involving only the mesoscopic particles, this property holds if the counterions are traced out in the partition function and colloidal particles are assumed to interact with the exact effective one-component Hamiltonian. Since the complexity of the mixture is preserved in the exact effective one-component Hamiltonian, one needs to resort to approximations in order to find a simple expression for this quantity. The replacement of the exact effective one-component Hamiltonian by an approximate effective one-component Hamiltonian with pairwise state-dependent DLVO interactions $V(r; \rho, T)$ has, however, deep consequences. It is worth noting that in the approximate effective one-component description we have a short-

ranged colloid–colloid pcf all over the phase diagram because of the repulsive nature of the DLVO potential. This is indeed a poor approximation for the colloid–colloid pcf in the mixture when a spinodal line or the critical point is approached, although away from the coexistence region the approximate pcf may be a quite good approximation of the exact pcf. Nevertheless we have shown that, even without including the volume term, HNC–DLVO captures a vapour–liquid transition indicating that the density dependence of the DLVO potential is responsible for driving the fluid towards the phase separation. By increasing the radius of the colloidal particle, this phase separation is dominated by the volume term, the DLVO screening mechanism playing only a minor role. Unfortunately, we have been unable to determine the vapour–liquid transition within CGHNC in order to compare it to the phase separation resulting from HNC–DLVO.

In this paper we have also analysed the thermodynamics resulting from the DLVO theory (1). The procedure outlined here follows the standard methods in equilibrium statistical mechanics. From the approximate effective one-component Hamiltonian, one first determines the Helmholtz free energy, the remaining thermodynamic quantities being found using elementary thermodynamic relations. This is the only way to guarantee a self-consistent thermodynamics within the effective one-component description. We have shown that (when discarding the volume term) the virial and the energy equations look like their atomic counterparts but with different state-dependent potentials $V_{\mathrm{p}}(r;\,\rho,\,T)$ and $V_{\mathrm{u}}(r;\,\rho,\,T)$. Despite the purely repulsive nature of the DLVO potential, both $V_{\mathrm{p}}(r;\,\rho,\,T)$ and $V_{\mathrm{u}}(r;\,\rho,\,T)$ contain an attractive contribution. The long-ranged attraction in $V_{\mathrm{p}}(r;\,\rho,\,T)$ agrees with the classical van der Waals picture and the virial equation reproduces the HNC–DLVO vapour–liquid transition. As a consequence, the standard compressibility equation no longer holds in the effective one-component description. We point out that the basic principle of the compressibility equation for atomic fluids involves a charging process of the density at constant interactions [7]. For the DLVO potential when the fluid is charged with respect to the density it is simultaneously charged with respect to the interactions and this explains why the compressibility equation has also to be modified in order to yield a self-consistent thermodynamics [12]. Therefore, using the virial, the energy and the compressibility equations for atomic fluids in the effective one-component description would lead to thermodynamical inconsistencies [16].

In summary, the DLVO theory provides an effective one-component description which captures most of the experimental and simulation topics of charge-stabilized colloidal suspensions. The price to be paid is that the well established equations for atomic fluids have to be modified.

Acknowledgments

We are grateful to M Dijkstra and R van Roij for sending to us their simulation results. We wish to thank M Baus and E Lomba for many useful discussions. We acknowledge financial support from the Dirección General de Enseñanza Superior e Investigación Científica (DGESCYT) under grants No BFM2001-1017-C03-03 (GR and CFT) and No BQU2001-3615-C02-01 (JAA) and from the Instituto de Salud Carlos III grant No 01/1664 (JAA).

References

[1] See e.g. Poon W C K and Pusey P N 1995 *Observation, Prediction and Simulation of Phase Transitions in Complex Fluids* ed M Baus, L F Rull and J P Ryckaert (Dordrecht: Kluwer)

[2] Likos C N 2001 *Phys. Rep.* **348** 267

[3] van Roij R, Dijkstra M and Hansen J P 1999 *Phys. Rev.* E **59** 2010
see also Denton A R 2000 *Phys. Rev.* E **62** 3855

[4] Verwey J W and Overbeek J Th G 1948 *Theory of the Stability of Lyotropic Colloids* (Amsterdam: Elsevier)
[5] Crocker J C and Grier D G 1994 *Phys. Rev. Lett.* **73** 352
Kepler G M and Fraden S 1994 *Phys. Rev. Lett.* **73** 356
Crocker J C and Grier D G 1996 *Phys. Rev. Lett.* **77** 1897
[6] Tata B R V, Rajalakshmi M and Arora A K 1992 *Phys. Rev. Lett.* **69** 3778
Larsen A E and Grier D G 1996 *Phys. Rev. Lett.* **76** 3862
Larsen A E and Grier D G 1997 *Nature* **385** 230
[7] Evans R 1979 *Adv. Phys.* **28** 143
[8] Ascarelli P and Harrison R 1969 *Phys. Rev. Lett.* **22** 285
[9] Robbins M O, Kremer K and Grest G G 1988 *J. Chem. Phys.* **88** 3286
Thimuralai D 1989 *J. Phys. Chem.* **93** 5637
Meijer E J and Frenkel D 1991 *J. Chem. Phys.* **94** 2269
Dupont G, Moulinasse S, Ryckaert J P and Baus M 1993 *Mol. Phys.* **79** 453
[10] Dijkstra M and van Roij R 1998 *J. Phys.: Condens. Matter* **10** 1219
[11] Gray C G and Gubbins K E 1984 *Theory of Molecular Fluids* (Oxford: Clarendon)
[12] Tejero C F 2003 *J. Phys.: Condens. Matter* **15** S395
Tejero C F and Baus M 2003 *J. Chem. Phys.* **118** 892
[13] Belloni L 1986 *Phys. Rev. Lett.* **57** 2026
[14] Anta J A and Lago S 2002 *J. Chem. Phys.* **116** 10514
see also Anta J A, Bresme F and Lago S 2003 *J. Phys.: Condens. Matter* **15** S3491
[15] Belloni L 2000 *J. Phys.: Condens. Matter* **12** R549
[16] Louis A A 2002 *J. Phys.: Condens. Matter* **14** 9187